ICJK
Journal of Advanced Materials Research
http://dx.doi.org/10.62762/JAMR.2026.956976

RESEARCH ARTICLE

Microstructure and Optical Properties of BaF_2 Transparent Ceramics Fabricated by Air Pre-sintering and Hot Isostatic Pressing

Heng Liu[1,3], Chen Hu[1,2,*], Jingshan Hou[3], Ziqiu Cheng[1,2], Junhao Ye[1,2], Tingsong Li[1,2], Dong Huang[1], Yongzheng Fang[3,*], Dariusz Hreniak[4] and Jiang Li[1,2,*]

[1] State Key Laboratory of High Performance Ceramics, Shanghai Institute of Ceramics, Chinese Academy of Sciences, Shanghai 201899, China
[2] Center of Materials Science and Optoelectronics Engineering, University of Chinese Academy of Sciences, Beijing 100049, China
[3] School of Materials Science and Engineering, Shanghai Institute of Technology, Shanghai 201418, China
[4] Institute of Low Temperature and Structure Research, Polish Academy of Sciences, Wrocław 50-422, Poland

Abstract

BaF_2 scintillation ceramics feature a rapid temporal response, high fast-component light yield, and a short X-ray attenuation length, making them a promising material for ultrafast X-ray imaging. In this work, BaF_2 nanopowder was co-precipitated from $Ba(NO_3)_2$ and $KF{\cdot}2H_2O$, consolidated by 600–750 °C air pre-sintering, and post-treated by hot isostatic pressing (HIP). The ceramics obtained under various process parameters allowed us to investigate temperature-dependent changes in microstructure, transmittance, and scintillation properties, including X-ray-excited luminescence (XEL), decay kinetics, and light yield. It was found that air pre-sintered compacts are porous, with relative density reaching a maximum at 700 °C. In addition, HIP eliminated most of the pores, leaving only residual intragranular pores. Both in-line transmittance and scintillation properties correlated strongly with increasing air pre-sintering temperature. The optimized BaF_2 ceramic achieves an in-line transmittance (1 mm thick) of 57.6% and 40.6% at 800 nm and 220 nm, respectively, with a fast component of 16.8% and a light yield of 2655 ph/MeV. High-temperature thermoluminescence suggests that a deep trap with considerable intensity may be responsible for the reduced light yield in the ceramic sample.

Keywords: BaF_2 scintillation ceramics, Microstructure, Scintillation properties, Hot isostatic pressing.

Submitted: 29 June 2026
Revised: 29 August 2026
Accepted: 03 September 2026
Published: 08 September 2026

Vol. 2, **No.** 4, 2026.
10.62762/JAMR.2026.956976

***Corresponding authors:**
✉ Chen Hu
huchen@mail.sic.ac.cn
✉ Yongzheng Fang
fyz1003@sina.com
✉ Jiang Li
lijiang@mail.sic.ac.cn

Citation
Liu, H., Hu, C., Hou, J., Cheng, Z., Ye, J., Li, T., Huang, D., Fang, Y., Hreniak, D., & Li, J. (2026). Microstructure and Optical Properties of BaF_2 Transparent Ceramics Fabricated by Air Pre-sintering and Hot Isostatic Pressing. *Journal of Advanced Materials Research*, 2(4), 262–273.

© 2026 by the Authors. Published by Institute of Central Computation and Knowledge. This is an open access article under the CC BY license (https://creativecommons.org/licenses/by/4.0/).

1 Introduction

As experiments in high-energy physics (HEP) advance towards higher energies and event rates [1–4] and the demand for temporal resolution in medical imaging continues to grow, ultrafast imaging and time measurement technologies have become core frontiers in contemporary physics and precision medicine. These future experiments face unprecedented challenges related to the event rates and extreme radiation environments, requiring detector systems to respond in less than a sub-nanosecond or even a picosecond [5, 6]. Various scintillators and Cherenkov radiators have been explored as candidate materials for such timing detectors, underscoring the breadth of the instrumentation challenge [7]. In the field of medical imaging, time-of-flight positron emission tomography (TOF-PET) determines the spatial location of annihilation events by precisely measuring the time difference of arrival of annihilation photon pairs at the detectors, and its effective sensitivity is directly related to the coincidence time resolution (CTR)—the smaller the CTR, the higher the image signal-to-noise ratio and the more accurate the spatial positioning [8, 9]. The design of data acquisition setups plays a critical role in exploiting the fast timing capability of scintillators in practical TOF-PET systems [10]. In addition, gigahertz (GHz) hard X-ray imaging, as an emerging ultrafast imaging technology, also poses unprecedented challenges to the speed and radiation tolerance of front-end detector materials [5, 6, 11, 12]. Recent advances have shown that rare-earth-doped perovskite scintillators can achieve sub-nanosecond time resolution and GHz-level repetition frequency detection capability [13]; however, their relatively poor radiation hardness and limited scalability underscore the continued need for large-scale inorganic ceramic alternatives such as BaF_2.

The common core requirement of the ultrafast imaging applications is that the detector front-end needs an inorganic scintillator that combines an ultrafast scintillation response with high radiation resistance. Since the achievable optimal temporal resolution is proportional to the square root of the scintillation decay time [14, 15], shortening the scintillation decay time is a direct way to overcome the limitation of time resolution. Although LYSO:Ce is widely used in PET systems among mainstream inorganic scintillators owing to its high density and high light yield [16], its decay time of approximately 40 ns limits the potential for further improving time resolution [17]. Efforts to further enhance the light yield of LYSO:Ce through co-doping strategies, such as trace Co^{2+} incorporation, have demonstrated substantial improvements but do not address the fundamental limitation of its long decay time [18].

Among all the fast and ultrafast scintillators, barium fluoride (BaF_2) stands out due to its unique cross-luminescence mechanism. The fast scintillation component of BaF_2 emits in the deep ultraviolet region (195 nm and 220 nm) with an ultrafast decay time of ~0.6 ns, which is one of the fastest known inorganic scintillators [19–23]. However, BaF_2 materials still face two major challenges in practical applications. Firstly, in addition to the fast cross-luminescence component, BaF_2 also has a slow component with a peak at 310 nm and a decay time of about 600 ns. This slow component originates from the radiative recombination of self-trapped excitons and can cause serious signal pile-up issues in high count rate applications [24, 25]. Doping with rare earth ions (such as Y, La, Ce, etc.) can effectively suppress the slow component—for example, 1 at% Y doping can suppress the slow component of BaF_2 by six times without affecting the fast component [26–29]. The second challenge is that the growth of BaF_2 single crystals is costly and size-limited, making it difficult to meet the mass production requirements for large-area detector arrays [22, 24].

Thanks to the advancement in nano-powder synthesis via co-precipitation [30, 31] and ceramic fabrication technology [32–36], polycrystalline transparent ceramics provide a highly promising technical pathway to address the two bottlenecks mentioned above. Beyond polycrystalline sintered ceramics, related fluoride-based scintillator materials such as CaF_2:Tb^{3+} transparent glass-ceramics have also demonstrated promising anti-thermal-quenching luminescence for high-temperature X-ray imaging [37], further illustrating the broad potential of fluoride ceramic scintillators and motivating systematic study of the BaF_2 ceramic system. Compared to single crystals, ceramics offer significant advantages such as lower processing temperatures, the ability to form large sizes and complex shapes, and easier control over doping concentration and uniformity [25, 31]. In recent years, preliminary progress has been made in the preparation of BaF_2 transparent ceramics and the study of their scintillation properties. Kato et al. [38] fabricated BaF_2 transparent ceramics using spark plasma sintering (SPS) and evaluated their scintillation performance. Li et al. [39] synthesized Nd:BaF_2 nano-powders via co-precipitation and

fabricated transparent ceramics by vacuum sintering, achieving a transmittance of approximately 70% in the infrared range. Liu et al. [31, 40] synthesized Pr^{3+}:BaF_2 nano-powders via co-precipitation and prepared transparent ceramics with a transmittance of 50.7% at 500 nm by hot-pressing at 900 °C and 50 MPa for 4 hours; however, residual pores remained the main source of light scattering. Liu et al. [41] also reported a new attempt to prepare translucent BaF_2 ceramics using a one-step cold sintering method. Li et al. [24] prepared BaF_2 transparent ceramics by hot-pressing combined with hot isostatic pressing (HIP) post-treatment and, by comparing with BaF_2 single crystals, found that the fast-quenching centers present in the ceramics can effectively quench self-trapped excitons (STE), thereby significantly suppressing the slow scintillation component. Beyond the BaF_2 system, radiation response properties of other fluoride transparent ceramics such as Ce:CaF_2 have also been systematically evaluated, further confirming the potential of ceramic scintillators for radiation detection applications [42]. Nevertheless, existing methods still face challenges in eliminating residual pores and improving optical quality and scintillation performance.

In the field of fluoride transparent ceramic fabrication, a two-step process combining air pre-sintering with HIP post-treatment has shown significant advantages in the CaF_2 and SrF_2 systems. Huang et al. [43] and Liu et al. [44] used this method to prepare Yb,La:CaF_2 and Yb:CaF_2 transparent ceramics, respectively, and achieved laser output. Li et al. [45] further optimized the process parameters for Yb:CaF_2 ceramics, demonstrating that calcination temperature of co-precipitated powders critically governs both microstructure and laser performance. Liu et al. demonstrated the feasibility of Er:SrF_2 transparent ceramic fabrication using chemically derived powders [46], and Feng et al. further extended the air pre-sintering and HIP route to the Er:SrF_2 system [47]. This method allows the green body to reach preliminary densification at the closed-pore stage through air pre-sintering, after which HIP post-treatment efficiently eliminates residual closed pores using uniform isostatic pressure, ultimately obtaining ceramics with near-theoretical density and high optical quality. However, for the BaF_2 scintillator ceramic system, systematic research on this process route is still lacking.

Based on this, in this work, BaF_2 nano-powders were synthesized by the co-precipitation method. For the first time, a two-step process combining air pre-sintering with HIP post-treatment was used to prepare BaF_2 scintillation ceramics. The study systematically investigated the effects of air pre-sintering temperature on ceramic phase, microstructure, and density, as well as the effects of HIP treatment on ceramic microstructure, optical quality, and scintillation performance. Finally, high-temperature thermoluminescence was used to analyze the structural defects in the prepared ceramics.

2 Experimental

BaF_2 nano-powders were prepared by the co-precipitation method, using high-purity commercial reagents $Ba(NO_3)_2$ (AR, China National Pharmaceutical Group Chemical Reagent Co., Ltd.) and $KF{\cdot}2H_2O$ (AR, China National Pharmaceutical Group Chemical Reagent Co., Ltd.) as raw materials. Solutions of a certain concentration of reagents were prepared separately using deionized water and purified by vacuum filtration. To ensure complete precipitation of BaF_2 and to increase the yield of the powder synthesis process, the concentration of the KF solution was controlled to be 2.5 times that of the $Ba(NO_3)_2$ solution. The KF solution was added dropwise to the continuously stirred $Ba(NO_3)_2$ solution at a rate of 6 mL/min using a constant-flow peristaltic pump. After titration, the resulting precipitate was left at room temperature for 12 hours, then washed three times with deionized water to thoroughly remove residual NO_3^- and K^+ ions. The washed product was first stored at −50 °C for 10 hours, then transferred to a freeze dryer (Scientz-10N, Ningbo Scientz Biotech Co., Ltd.) and dried under 10 Pa for 12 hours. Finally, the dried powder was passed through a 200-mesh sieve (mesh size about 0.075 mm) to obtain BaF_2 nano-powder suitable for subsequent sintering.

The synthesized nano-powder was uniaxially pressed at 20 MPa, followed by cold isostatic pressing at 250 MPa. The green body was pre-sintered at a temperature of 600–750 °C in air for 2 hours. Then, the pre-sintered body was hot isostatically pressed at 800 °C under 100 MPa in an Ar atmosphere for 3 hours. The BaF_2 ceramics obtained by sintering were processed into pellets with a diameter of Φ13.5 mm and double-side polished to a thickness of 2 mm for scintillation performance characterization, and then polished again to a thickness of 1 mm for in-line transmittance measurement.

The phase composition of the synthesized powders was analyzed using an X-ray diffractometer (XRD, D8 Advance, Bruker, Germany). The microstructure of the powders and the ceramic fracture surfaces was observed with a field emission scanning electron microscope (FESEM; SU8220, Hitachi, Japan). The relative density of the ceramics was tested using the Archimedes drainage method. The in-line transmittance of the ceramic samples was measured in the wavelength range of 200–800 nm using a UV-Vis-NIR spectrophotometer (Cary5000, Varian, USA).

X-ray excited luminescence (XEL) spectroscopy measurement was performed using a home-built XEL spectroscopy system. This system uses an F30III-2 X-ray tube (tungsten anode, operating conditions: 75 kV/1.3 mA) as the excitation source, and the luminescence signal is collected via a fiber optic coupled to a QE65000 spectrometer (Ocean Optics).

In the scintillation decay time and light yield tests, the ceramic and single crystal samples were optically coupled to a photomultiplier tube (PMT; R2059, Hamamatsu) window using silicone grease, and multiple layers of Teflon film were wrapped around the samples to effectively guide the scintillation photons into the PMT's photosensitive cathode. The scintillation decay curves were excited by a ^{137}Cs radiation source, received by the same PMT R2059, and digitally recorded by a digital oscilloscope (TBS1106, Tektronix).

In the measurement of light yield, the scintillation light generated when the sample is irradiated by a radiation source is converted into an electrical signal by the PMT R2059. This signal is then amplified and shaped sequentially by a preamplifier (ORTEC 113) and a main amplifier (ORTEC 671), followed by collecting the energy spectrum through a multichannel analyzer (Trump-PCI 2k MCA, ORTEC) and reading the multichannel spectrum data using ORTEC Maestro software. By performing Gaussian fitting on the full-energy peak and combining it with the single photoelectron calibration method, the light yield is calculated.

Thermally stimulated luminescence (TSL) measurements were carried out to analyze defects in a sample by recording the luminescence of the material during temperature changes. For high-temperature thermoluminescence above room temperature, an SL08 thermoluminescence measurement instrument (Guangzhou Rongfan Technology Co., Ltd.) was used to uniformly heat the sample (heating rate of 2 K/s), and the thermoluminescence signal was simultaneously recorded during the heating process.

3 Results and discussion

Figure 1 shows the FESEM morphology of BaF_2 nano-powders synthesized by the chemical co-precipitation method. The synthesized powders are mainly composed of thick plate-like particles, with a relatively regular morphology and slight agglomeration. The primary particles exhibit a cubic structure because BaF_2 has a cubic crystal system, which tends to grow into a cubic shape during the co-precipitation process.

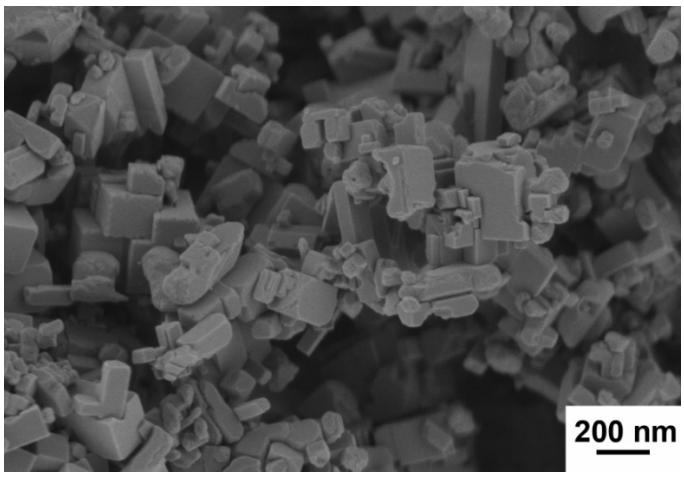


Figure 1. FESEM micrograph of BaF_2 nano-powders synthesized via the chemical co-precipitation method.

Figure 2 shows the XRD patterns of BaF_2 ceramics obtained by air pre-sintering in the range of 600–750 °C for 2 hours. By comparing with the XRD Powder Diffraction File database (PDF#04-0452), it can be seen that ceramics prepared at different pre-sintering temperatures all exhibit a pure cubic BaF_2 phase, and no secondary phase was detected. This indicates that during the air pre-sintering process, no obvious reaction of the BaF_2 ceramic green bodies with O_2 or H_2O in the air occurs at these temperatures, and no oxide or hydroxide impurities were formed.

Figure 3 shows the FESEM microstructure of the cross-section of BaF_2 ceramics prepared by air pre-sintering (600–750 °C × 2 h). Under the pre-sintering condition of 600 °C, the ceramic is at the initial stage of densification, with numerous interconnected open pores between grains, small and unevenly distributed grain sizes, and overall low densification. As the pre-sintering temperature increases to 650–700 °C, the number of pores

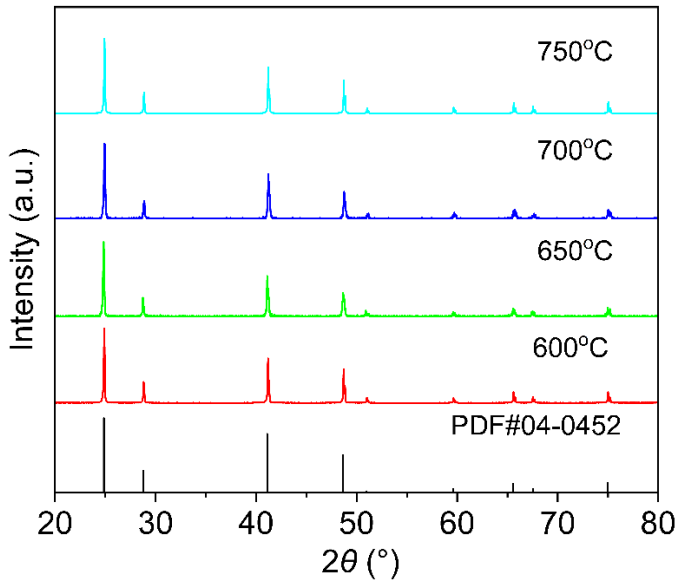


Figure 2. XRD patterns of the BaF_2 ceramics pre-sintered in air at 600–750 °C for 2 h.

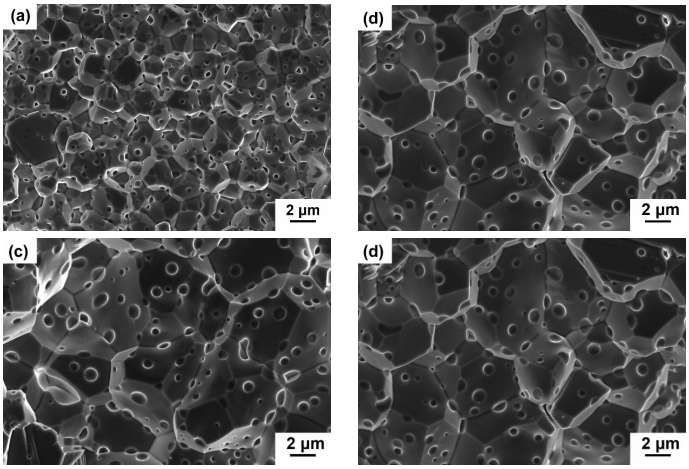


Figure 3. FESEM micrographs of fracture surfaces of BaF_2 scintillation ceramics prepared by air pre-sintering at different temperatures for 2 h: (a) 600 °C, (b) 650 °C, (c) 700 °C and (d) 750 °C.

significantly decreases, grains grow noticeably, grain boundaries gradually become clear, and the degree of densification continues to improve. When the pre-sintering temperature further rises to 750 °C, the grain growth rate significantly accelerates, grain size increases substantially, and some pores are enclosed by rapidly growing grains, forming intragranular pores.

Figure 4 shows the densification curve of the same BaF_2 ceramic samples. As can be seen, the relative density of the ceramics first increases and then decreases with the sintering temperature: when the pre-sintering temperature rises from 600 °C to 700 °C, the relative density increases from 95.5% to 96.7%; upon further increasing to 750 °C, the density drops back to 95.4% owing to the formation of intragranular pores. The overall density of the air pre-sintered samples is not high, and a large number of pores still exist within the ceramic (as can be seen in Figure 3). Therefore, post-treatment via HIP is required to further eliminate pores and improve the degree of densification.

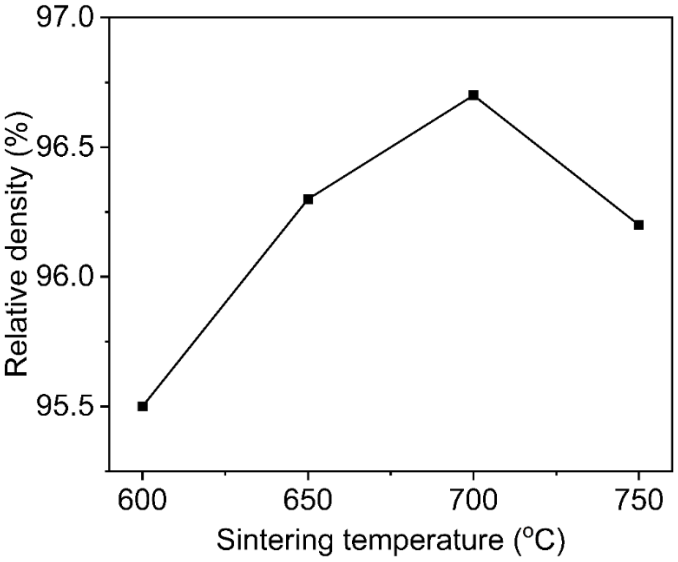


Figure 4. Relative density curves of the BaF_2 ceramics pre-sintered in air at 600–750 °C for 2 h.

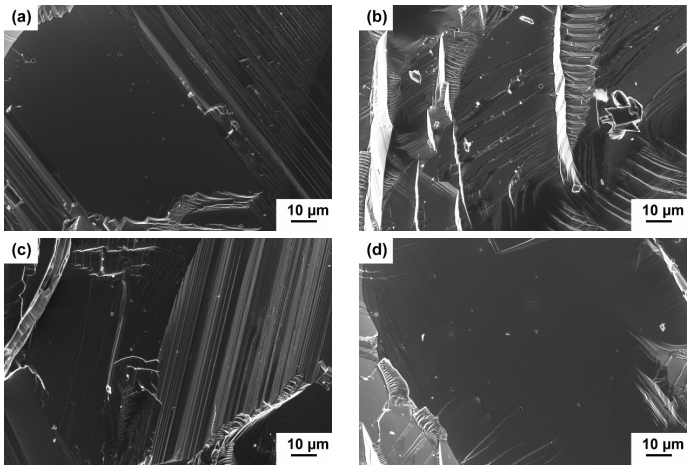


Figure 5. FESEM micrographs of fracture surfaces of BaF_2 scintillation ceramics pre-sintered in air at different temperatures for 2 h and HIP post-treated at 800 °C for 3 h under 100 MPa Ar: (a) 600 °C, (b) 650 °C, (c) 700 °C and (d) 750 °C.

Figure 5 shows the FESEM microstructure of the ceramic cross-section prepared by air pre-sintering (600–750 °C × 2 h) combined with HIP post-treatment (800 °C × 3 h, 100 MPa Ar). After HIP treatment at 800 °C, compared with before HIP, the number of internal pores greatly decreased, leaving only a few intragranular pores. The intragranular pores may be formed during the pre-sintering process, when

the grain boundary growth rate is faster than the pore elimination rate, and this phenomenon becomes pronounced when the pre-sintering temperature reaches 750 °C. Therefore, when the air pre-sintering temperature is 750 °C, obvious intragranular pores appear in the ceramics, which are difficult to remove even after the HIP post-treatment.

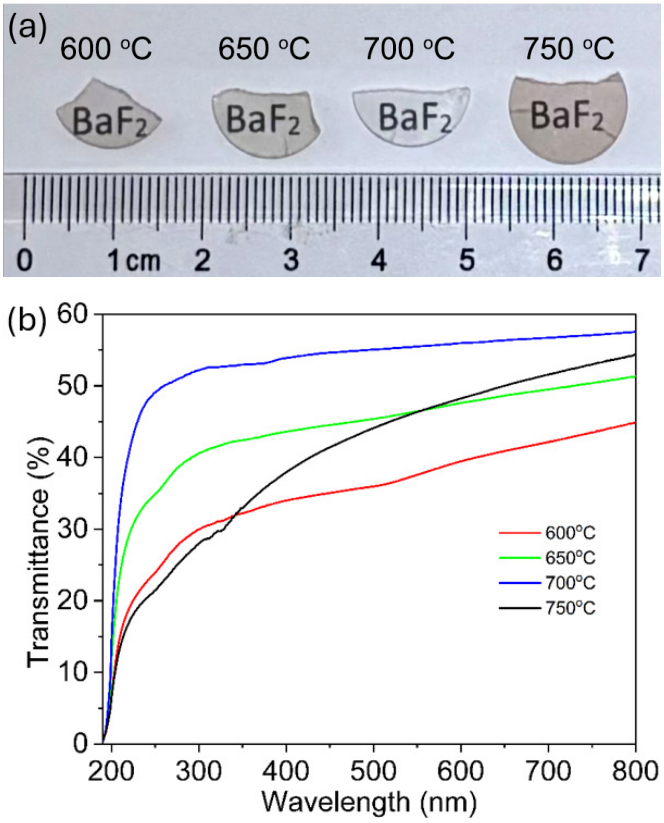


Figure 6. (a) Photograph and (b) in-line transmittance curves of BaF_2 scintillation ceramics pre-sintered in air at 600–750 °C for 2 h and HIP post-treated at 800 °C for 3 h under 100 MPa Ar (1 mm in thickness).

Figure 6 shows (a) a photograph and (b) in-line transmittance curves of BaF_2 scintillation ceramics (1 mm thick) prepared by air pre-sintering (600–750 °C × 2 h) combined with HIP post-treatment (800 °C × 3 h, 100 MPa Ar). While the sample air pre-sintered at 700 °C is colorless and transparent, the sample air pre-sintered at 750 °C shows a reddish color. With the increase of air pre-sintering temperature, the in-line transmittance of the HIP-treated BaF_2 ceramics generally shows a trend of first increasing and then decreasing, which is consistent with the changes in the number of pores and relative density in the ceramics. The in-line transmittance of BaF_2 scintillation ceramics prepared by air pre-sintering (700 °C × 2 h) combined with HIP post-treatment (800 °C × 3 h, 100 MPa Ar) is 57.6% at 800 nm and 40.6% at 220 nm, respectively.

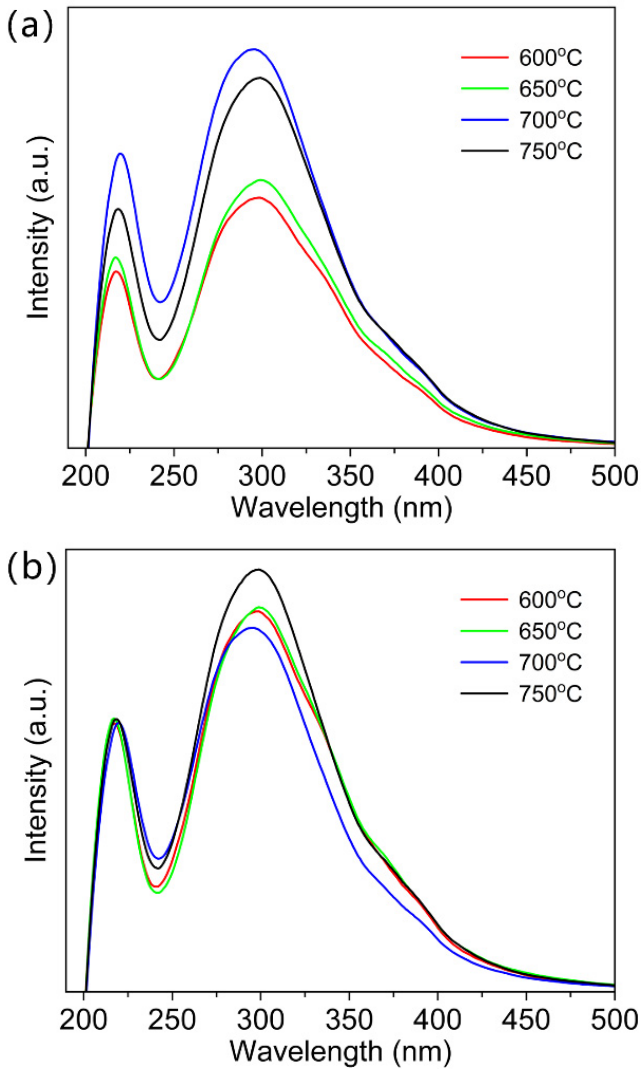


Figure 7. (a) XEL and (b) normalized XEL spectra of BaF_2 scintillation ceramics pre-sintered in air at 600–750 °C for 2 h and HIP post-treated at 800 °C for 3 h under 100 MPa Ar.

Figure 7(a) shows the XEL spectra of BaF_2 scintillation ceramics prepared by air pre-sintering (600–750 °C × 2 h) combined with HIP post-treatment (800 °C × 3 h, 100 MPa Ar). It can be seen that all samples exhibit two distinct emission peaks at approximately 220 nm and 310 nm, corresponding to cross-luminescence (CL) and self-trapped excitons (STE), respectively. The CL intensity initially increases and then decreases as the pre-sintering temperature rises. The highest CL intensity was obtained by the sample pre-sintered at 700 °C. To verify the suppression effect of STE luminescence in BaF_2 ceramics, the fast luminescence band was normalized, and the results are shown in Figure 7(b). As the air pre-sintering temperature increases, the suppression of the slow luminescence component at 310 nm caused by STE luminescence in BaF_2 scintillation ceramics first enhances and then weakens.

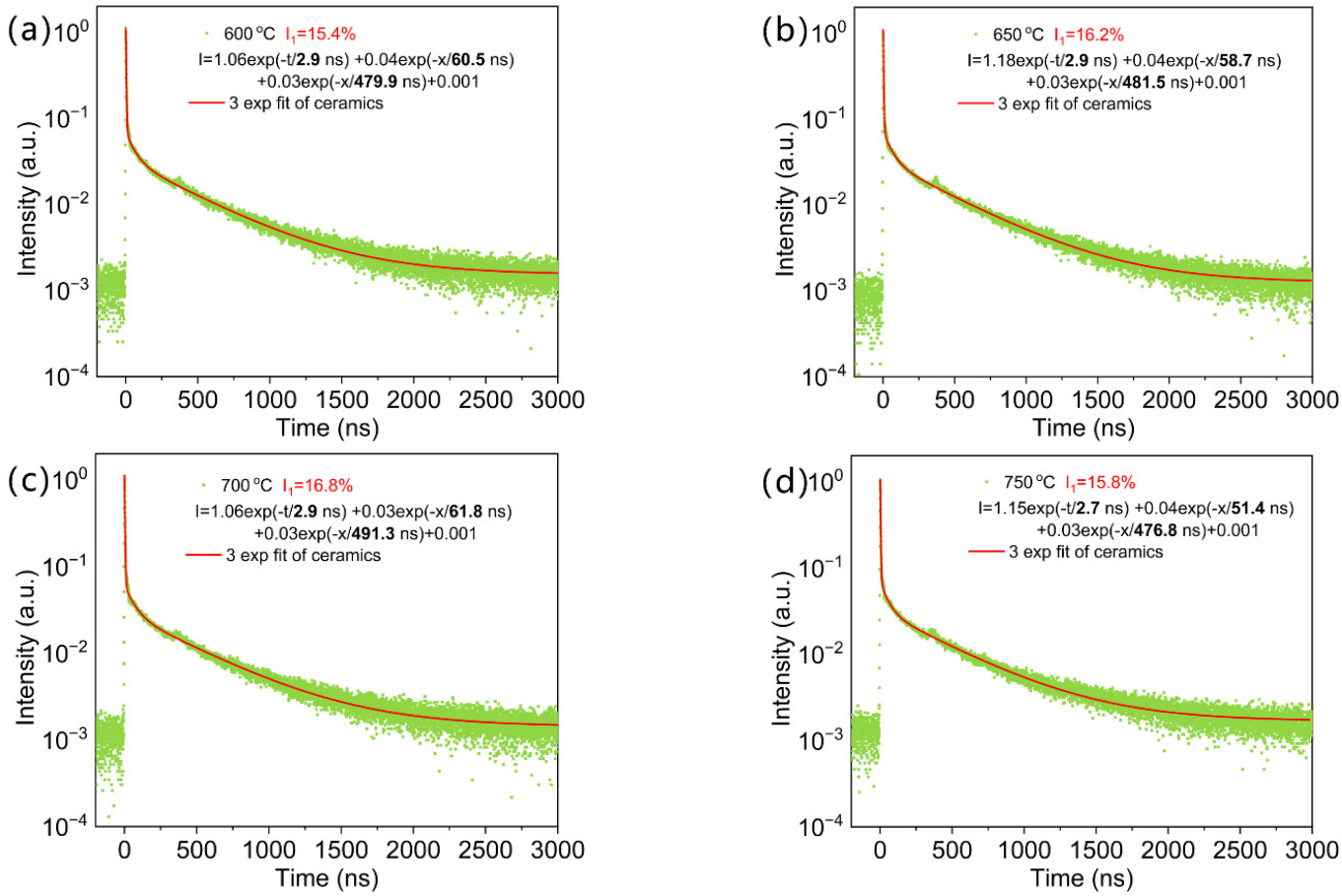


Figure 8. Scintillation decay curves of BaF_2 scintillation ceramics pre-sintered in air at different temperatures for 2 h and HIP post-treated at 800 °C for 3 h under 100 MPa Ar: (a) 600 °C, (b) 650 °C, (c) 700 °C, (d) 750 °C.

In order to further verify the reliability of the trend observed in the normalized XEL spectra, where the slow luminescence in BaF_2 scintillation ceramics is initially enhanced and then reduced, the scintillation decay time of BaF_2 scintillation ceramics was further evaluated. Figure 8 shows the scintillation decay curves of BaF_2 scintillation ceramics prepared by air pre-sintering (600–750 °C × 2 h) combined with HIP post-treatment (800 °C × 3 h, 100 MPa Ar). The decay curves of BaF_2 ceramics were fitted using a triple-exponential function [48]:

$$I = A_1 \exp\left(\frac{-t}{\tau_1}\right) + A_2 \exp\left(\frac{-t}{\tau_2}\right) + A_3 \exp\left(\frac{-t}{\tau_3}\right) + \text{background} \quad (1)$$

In the formula, τ_1 is the fast decay time constant obtained from fitting, τ_2 and τ_3 are the slow decay time constants obtained from fitting, and A_1, A_2 and A_3 are the corresponding amplitudes; the intensity proportion of the fast component I_1 is calculated by Eq. (2):

$$I_1 = A_1\tau_1 \Big/ \sum_n A_n\tau_n \quad (2)$$

The proportion of the fast component I_1 of BaF_2 scintillator ceramics calculated according to Eq. (2) is shown in Figure 8. The results indicate that the air pre-sintering temperature has a certain regulatory effect on the fast scintillation component of BaF_2 ceramics. As the sintering temperature increases from 600 °C to 700 °C, the proportion of the fast component gradually rises from 15.4% to 16.8%. When the temperature is further increased to 750 °C, the proportion of the fast component decreases to 15.8%, showing an overall trend of first increasing and then decreasing.

Figure 9 shows the pulse height spectra of BaF_2 scintillation ceramics prepared by air pre-sintering (700 °C × 2 h) combined with HIP post-treatment (800 °C × 3 h, 100 MPa Ar). The results demonstrate that a light output (L.O.) of 581 p.e./MeV and a light yield (L.Y.) of 2655 ph/MeV were obtained for the sample. These values are lower than

those of BaF_2 single crystals measured under identical conditions [24]. The reasons mainly include three aspects: firstly, various possible defects within the ceramics could capture carriers during the transport process, reducing the light yield; secondly, the ceramics' suppression of the slow scintillation component reduces the total light emission contribution; thirdly, the poor optical quality of the ceramics decreases the light output and collection efficiency. These three factors collectively contribute to the reduced light output and collection efficiency observed in the ceramic samples. Therefore, high-temperature TSL testing is required to further analyze the internal defect structure and clarify the cause of the light yield reduction.

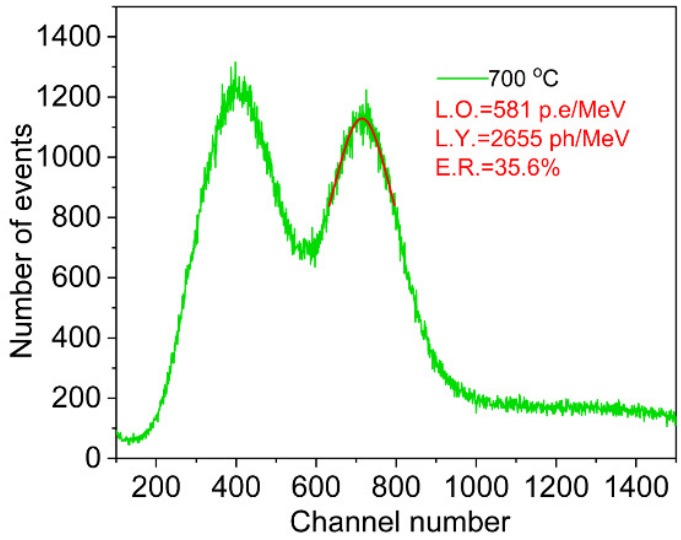


Figure 9. Pulse height spectra of the BaF_2 scintillation ceramic pre-sintered in air at 700 °C for 2 h and HIP post-treated at 800 °C for 3 h under 100 MPa Ar.

To elucidate why the BaF_2 scintillation ceramic exhibits a significantly lower light yield than its single-crystal counterpart, high-temperature TSL characterization was carried out. The results are shown in Figure 10. The integrated TSL intensity of BaF_2 ceramics can be fitted using the general-order kinetics equation [24, 49]:

$$I(T) = I_m b^{\frac{b}{b-1}} \exp\left(\frac{E}{kT}\frac{T-T_m}{T_m}\right)\left[(b-1)\left(1-\frac{2kT}{E}\right)\frac{T^2}{T_m^2} \times \exp\left(\frac{E}{kT}\frac{T-T_m}{T_m}\right) + 1 + (b-1)\frac{2kT_m}{E}\right]^{-\frac{b}{b-1}} \quad (3)$$

In the equation, I_m and T_m represent the peak intensity and peak temperature, respectively; k is the Boltzmann constant; b is the kinetic order; and E is the trap depth.

The TSL curves of all ceramic samples can be fitted and decomposed into three characteristic trap energy levels: $E_{T_1} = 0.80 \pm 0.08$ eV, $E_{T_2} = 1.16 \pm 0.12$ eV, and $E_{T_3} = 1.20 \pm 0.12$ eV. Among them, the 0.80 eV trap energy level is consistent with the trap energy level reported for BaF_2 single crystals [49], and it is speculated to be an intrinsic electron defect in the BaF_2 material. The trap energy levels of 1.16 eV and 1.20 eV are speculated, based on existing literature reports [50], to possibly correspond to lattice oxygen (O'_F) and barium vacancies (V''_{Ba}). Compared with the TSL glow curves of BaF_2 single crystals shown in the literature [49, 50], there is a very strong TSL peak above 650 K for the ceramic sample, which shows a much lower intensity in BaF_2 single crystals. This high-temperature TSL peak may be ascribed to some kind of deeper trap, which can seriously degrade the light yield of the ceramic sample.

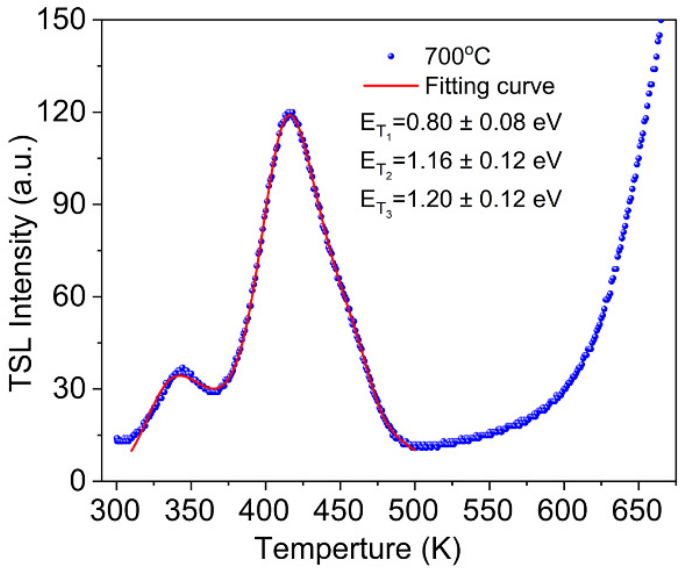


Figure 10. TSL and general-order fitting curve of the BaF_2 scintillation ceramic pre-sintered in air at 700 °C for 2 h and HIP post-treated at 800 °C for 3 h under 100 MPa Ar.

4 Conclusions

This work synthesized BaF_2 nano-powders using $Ba(NO_3)_2$ and $KF{\cdot}2H_2O$ as raw materials through a chemical co-precipitation method, and BaF_2 scintillation ceramics were prepared by air pre-sintering combined with HIP post-treatment. The effects of air pre-sintering temperature and HIP post-treatment on the phase, microstructure, and in-line transmittance of BaF_2 ceramics were investigated. The results show that the pre-sintered ceramics are all pure cubic phase BaF_2, with a large number of internal pores. The relative density of the pre-sintered ceramics first increases and then

decreases with increasing sintering temperature. After HIP treatment, the internal pores of the ceramics are significantly reduced, but a small number of intragranular pores still remain, and the in-line transmittance of the HIP-treated BaF_2 ceramics presents a trend of first increasing and then decreasing with increasing pre-sintering temperature. BaF_2 scintillation ceramics prepared by air pre-sintering (700 °C × 2 h) combined with HIP post-treatment (800 °C × 3 h, 100 MPa Ar) achieve an in-line transmittance of 57.6% at 800 nm and 40.6% at 220 nm (1 mm thick). The fast luminescence XEL intensity is the highest for this sample, the slow component is significantly suppressed, the fast component accounts for 16.8%, and the light yield is 2655 ph/MeV. Furthermore, a high-temperature TSL study of the BaF_2 ceramic sample was conducted. The results indicate that it contains three characteristic trap energy levels: 0.80 eV, 1.16 eV, and 1.20 eV, which may correspond to an intrinsic electron defect in the BaF_2 material, lattice oxygen (O'_F), and barium vacancies (V''_{Ba}), respectively. Another deeper trap with much stronger intensity was also observed for the ceramic sample, which may degrade the light yield of the sample. This study not only provides a new preparation strategy to meet the urgent demand for high-performance BaF_2 scintillators in ultrafast imaging technology but also opens a new route for the low-cost, high-quality preparation of fluoride scintillation ceramics.

Data Availability Statement

Data will be made available on request.

Funding

This work was supported in part by the National Natural Science Foundation of China under Grant 52502156; in part by the International Partnership Program of Chinese Academy of Sciences under Grant 030GJHZ2024026FN; in part by the National Key R&D Program of China under Grant 2026YFE0150500; and in part by the Polish National Agency for Academic Exchange (NAWA) under the joint research projects between the Republic of Poland and China 2025, project no. BPN/BCH/2025/1/00039/U/00001.

Conflicts of Interest

Jiang Li served as an Associate Editor of the *Journal of Advanced Materials Research* at the time of manuscript submission. To ensure the integrity of the peer-review process, Jiang Li was not involved in the editorial handling, peer review, or decision-making process for this manuscript, which was handled independently by another editor. The remaining authors declare no conflicts of interest.

AI Use Statement

The authors declare that no generative AI was used in the preparation of this manuscript.

Ethical Approval and Consent to Participate

Not applicable.

References

[1] Zhu, R. Y. (2019, January). Ultrafast and radiation hard inorganic scintillators for future HEP experiments. In *Journal of Physics: Conference Series* (Vol. 1162, No. 1, p. 012022). IOP Publishing. [CrossRef]

[2] Dujardin, C., Auffray, E., Bourret-Courchesne, E., Dorenbos, P., Lecoq, P., Nikl, M., ... & Zhu, R. Y. (2018). Needs, trends, and advances in inorganic scintillators. *IEEE Transactions on Nuclear Science, 65*(8), 1977-1997. [CrossRef]

[3] Nikl, M., & Yoshikawa, A. (2015). Recent R&D trends in inorganic single-crystal scintillator materials for radiation detection. *Advanced Optical Materials, 3*(4), 463-481. [CrossRef]

[4] Zhang, L., & Zhu, R. Y. (2025). Progress of inorganic scintillators for future HEP experiments. In *EPJ Web of Conferences* (Vol. 320, p. 00062). EDP Sciences. [CrossRef]

[5] Lecoq, P., Morel, C., Prior, J. O., Visvikis, D., Gundacker, S., Auffray, E., ... & Benoit, M. (2020). Roadmap toward the 10 ps time-of-flight PET challenge. *Physics in Medicine & Biology, 65*(21), 21RM01. [CrossRef]

[6] Hu, C., Zhang, L., Zhu, R. Y., Chen, A., Wang, Z., Ying, L., & Yu, Z. (2018). Ultrafast inorganic scintillators for gigahertz hard X-ray imaging. *IEEE Transactions on Nuclear Science, 65*(8), 2097-2104. [CrossRef]

[7] Cala', R., Martinazzoli, L., Kratochwil, N., Frank, I., Salomoni, M., Pagano, F., ... & Auffray, E. (2025). Exploring scintillators and Cherenkov radiators for MIP timing detectors. *Journal of Instrumentation, 20*(04), P04004. [CrossRef]

[8] Pots, R. H., Auffray, E., & Gundacker, S. (2020). Exploiting cross-luminescence in BaF_2 for ultrafast timing applications using deep-ultraviolet sensitive HPK silicon photomultipliers. *Frontiers in Physics, 8*, 592875. [CrossRef]

[9] Herweg, K., Nadig, V., Schulz, V., & Gundacker, S. (2023). On the prospects of BaF_2 as a fast scintillator for

time-of-flight positron emission tomography systems. *IEEE transactions on radiation and plasma medical sciences, 7*(3), 241-252. [CrossRef]

[10] Latella, R., Gonzalez, A. J., Benlloch, J. M., Lecoq, P., & Konstantinou, G. (2024). Comparative analysis of data acquisition setups for fast timing in ToF-PET applications. *IEEE Transactions on Radiation and Plasma Medical Sciences, 8*(7), 743-751. [CrossRef]

[11] Wang, Z., Barnes, C. W., Kapustinsky, J. S., Morris, C. L., Nelson, R. O., Yang, F., ... & Zhu, R. Y. (2015, May). Thin scintillators for ultrafast hard X-ray imaging. In *Photon Counting Applications 2015* (Vol. 9504, pp. 104-114). SPIE. [CrossRef]

[12] Hu, C., Zhang, L., Zhu, R. Y., Demarteau, M., Wagner, R., Xia, L., ... & Smith, T. (2019). Ultrafast inorganic scintillator-based front imager for Gigahertz Hard X-ray imaging. *Nuclear Instruments and Methods in Physics Research Section A: Accelerators, Spectrometers, Detectors and Associated Equipment, 940*, 223-229. [CrossRef]

[13] Lu, Y. Y., Chen, Z. H., Zhang, Z. Y., Guo, Z., Zou, Y., Liu, H. G., Yang, F., Ding, D. Z., Wang, Y., & Tai, R. Z. (2026). Sub-nanometer time resolution and gigahertz-level repetition frequency detection capability achieved by rare-earth-doped perovskite ultrafast scintillation detectors. *Acta Physica Sinica, 75*(5), 050803. [CrossRef]

[14] Gundacker, S., Pots, R. H., Nepomnyashchikh, A., Radzhabov, E., Shendrik, R., Omelkov, S., ... & Auffray, E. (2021). Vacuum ultraviolet silicon photomultipliers applied to BaF2 cross-luminescence detection for high-rate ultrafast timing applications. *Physics in Medicine & Biology, 66*(11), 114002. [CrossRef]

[15] Seifert, S., van Dam, H. T., & Schaart, D. R. (2012). The lower bound on the timing resolution of scintillation detectors. *Physics in medicine and biology, 57*(7), 1797-1814. [CrossRef]

[16] Zheng, R., Chen, J. B., Liu, Y. L., Xiao, P., & Xie, Q. G. (2024). Advance in lutetium yttrium silicate scintillation crystal for all-digital PET. *CT Theory and Applications, 33*(4), 405-420. https://www.cttacn.org.cn/en/article/doi/10.15953/j.ctta.2024.014

[17] Pepin, C. M., Bérard, P., Perrot, A. L., Pépin, C., Houde, D., Lecomte, R., ... & Dautet, H. (2004). Properties of LYSO and recent LSO scintillators for phoswich PET detectors. *IEEE Transactions on Nuclear Science, 51*(3), 789-795. [CrossRef]

[18] Qiu, P., Li, M., Li, C., Zhang, A., Xue, Z., Zheng, X., ... & Ding, D. (2026). Substantial enhancement of light yield in LYSO: Ce crystals via trace Co^{2+} co-doping. *Chemical Engineering Journal*, 172884. [CrossRef]

[19] Dorenbos, P., De Haas, J. T. M., Visser, R., Van Eijk, C. W. E., & Hollander, R. W. (1993). Absolute light yield measurements on BaF/sub 2/crystals and the quantum efficiency of several photomultiplier tubes. *IEEE transactions on nuclear science, 40*(4), 424-430. [CrossRef]

[20] Khanin, V., Venevtsev, I., & Rodnyi, P. (2023). Recent advances in the study of core-valence luminescence (cross luminescence). Review. *Optical Materials, 136*, 113399. [CrossRef]

[21] Hou, Y. R., Chen, L. Y., Gao, F., Qian, S., & Ren, J. (2026). High-precision coincidence time resolution of BaF_2 crystals. *Nuclear Instruments and Methods in Physics Research Section A, 1087*, 171449. [CrossRef]

[22] Zhang, J., Li, J. H., Li, X., Xu, J. W., Zheng, L. L., & Chen, J. F. (2026). Growth and stress control of large-diameter barium fluoride crystals with heavy yttrium doping concentration for radiation detection. *Journal of Crystal Growth, 677*, 128460. [CrossRef]

[23] Shendrik, R., Radzhabov, E., Myasnikova, A., Pankratova, V., Šarakovskis, A., Nepomnyashchikh, A., ... & Pankratov, V. (2025). Ultrafast core-to-core luminescence in BaF_2-LaF_3 single crystals. *Scientific Reports, 15*(1), 26558. [CrossRef]

[24] Li, X., Hu, C., Guo, L. H., Ye, J. H., Zhang, Y. H., Xu, J. W., Wu, J. L., Liu, Q., Shi, Y., Chen, J. F., Li, T. S., & Li, J. (2025). Scintillation properties and slow component suppression mechanism of BaF_2 transparent ceramics. *Journal of the American Ceramic Society*, 108, 20469. [CrossRef]

[25] Ikesue, A., & Aung, Y. L. (2008). Ceramic laser materials. *Nature photonics, 2*(12), 721-727. [CrossRef]

[26] Hu, C., Xu, C., Zhang, L., Zhang, Q., & Zhu, R. Y. (2019). Development of yttrium-doped BaF_2 crystals for future HEP experiments. *IEEE Transactions on Nuclear Science, 66*(7), 1854-1860. [CrossRef]

[27] Zheng, J. Q., Chen, J. F., Li, X., Lu, B. Q., & Feng, H. (2022). Research progress on suppression of slow scintillation component in barium fluoride crystal by doping. *Journal of Synthetic Crystals, 51*(6), 951-964. https://www.researching.cn/articles/OJacef15f22818c026

[28] Hu, C., Zhang, L., Zhu, R. Y., Chen, A., Wang, Z., Ying, L., & Yu, Z. (2020). BaF2: Y and ZnO: Ga crystal scintillators for GHz hard X-ray imaging. *Nuclear Instruments and Methods in Physics Research Section A: Accelerators, Spectrometers, Detectors and Associated Equipment, 950*, 162767. [CrossRef]

[29] Schotanus, P., Dorenbos, P., Van Eijk, C. W. E., & Lamfers, H. J. (1989). Suppression of the slow scintillation light output of BaF_2 crystals by La^{3+} doping. *Nuclear Instruments and Methods in Physics Research Section A: Accelerators, Spectrometers, Detectors and Associated Equipment, 281*(1), 162-166. [CrossRef]

[30] Ye, J., Zhou, Z., Hu, C., Wang, Y., Jing, Y., Li, T., ... & LI, J. (2025). Yb: Sc 2 O 3 Transparent Ceramics Fabricated from Co-precipitated Nano-powders: Microstructure and Optical Property. *Journal of Inorganic Materials, 40*(2), 215-224. [CrossRef]

[31] Liu, X., Zhou, Z., Li, W., Yang, Y., & Mei, B. (2021). The effects of the solution reactant concentration and temperature on the preparation of Pr^{3+}: BaF_2

transparent ceramics. *Journal of the American Ceramic Society, 104*(8), 3862-3872. [CrossRef]

[32] Kawano, N., Kato, T., Nakauchi, D., Takebuchi, Y., Fukushima, H., Shiratori, D., ... & Yanagida, T. (2023). TSL, OSL and scintillation properties of Tb-doped barium fluoride translucent ceramics. *Optical Materials, 141*, 113948. [CrossRef]

[33] Greskovich, C., & Duclos, S. (1997). Ceramic scintillators. *Annual review of materials science, 27*(1), 69-88. [CrossRef]

[34] Wang, S. F., Zhang, J., Luo, D. W., Gu, F., Tang, D. Y., Dong, Z. L., ... & Kong, L. B. (2013). Transparent ceramics: Processing, materials and applications. *Progress in solid state chemistry, 41*(1-2), 20-54. [CrossRef]

[35] Chen, X., & Wu, Y. (2020). High concentration Ce3+ doped BaF2 transparent ceramics. *Journal of Alloys and Compounds, 817*, 153075. [CrossRef]

[36] Li, X., Hu, C., Liu, Q., Hreniak, D., & Li, J. (2024). Fluoride transparent ceramics for solid-state lasers: A review. *Journal of Advanced Ceramics, 13*, 1891-1918. [CrossRef]

[37] He, G. L., Jiang, G. H., Ren, S. B., Chen, J. Y., Li, L. J., & Guo, H. (2026). CaF_2:Tb^{3+} transparent glass-ceramic scintillators with anti-thermal-quenching luminescence for high-temperature X-ray imaging. *Journal of Rare Earths*. [CrossRef]

[38] Kato, T., Okada, G., Fukuda, K., & Yanagida, T. (2017). Development of BaF_2 transparent ceramics and evaluation of the scintillation properties. *Radiation Measurements, 106*, 140-145. [CrossRef]

[39] Li, J., Chen, X., Tang, L., Li, Y., & Wu, Y. (2019). Fabrication and properties of transparent Nd-doped BaF2 ceramics. *Journal of the American Ceramic Society, 102*(1), 178-184. [CrossRef]

[40] Liu, X., Tan, G., Zhou, Z., Li, W., Yang, Y., Sun, Z., & Mei, B. (2022). Effect of Pr3+ doping concentration on microstructure and optical properties of transparent BaF2 ceramics. *Journal of Alloys and Compounds, 895*, 162623. [CrossRef]

[41] Liu, B., Sha, K., Zhou, Q. W., Song, K. X., Shi, F., & Cheng, Y. H. (2023). One-step cold sintering process towards translucent BaF_2 ceramics. *Journal of the European Ceramic Society, 43*(15), 7053-7058. [CrossRef]

[42] Kawano, N., Kato, T., Conner, R. L., Jacobsohn, L. G., Nakauchi, D., Takebuchi, Y., ... & Yanagida, T. (2024). Radiation response properties of Ce-doped CaF2 transparent ceramics. *Materials Research Bulletin, 171*, 112609. [CrossRef]

[43] Huang, X. Y., Chen, G. M., Wei, J. B., Liu, Z. Y., Fang, Y. G., Tian, F., Xie, T. F., & Li, J. (2021). Fabrication of Yb,La:CaF_2 transparent ceramics by air pre-sintering with hot isostatic pressing. *Optical Materials, 116*, 111108. [CrossRef]

[44] Liu, Z. Y., Wei, J. B., Toci, G., Pirri, A., Patrizi, B., Feng, Y. G., Xie, T. F., Hreniak, D., Vannini, M., & Li, J. (2022). Microstructure and laser emission of Yb:CaF_2 transparent ceramics fabricated by air pre-sintering and hot isostatic pressing. *Optical Materials, 129*, 112540. [CrossRef]

[45] Li, X., Hu, C., Guo, L., Wu, J., Toci, G., Pirri, A., ... & Li, J. (2024). Optimization of Yb:CaF_2 transparent ceramics by air pre-sintering and hot isostatic pressing. *Ceramics, 7*(3), 1053-1065. [CrossRef]

[46] Liu, J., Liu, P., Wang, J., Xu, X., Li, D., Zhang, J., & Nie, X. (2018). Fabrication and sintering behavior of Er: SrF2 transparent ceramics using chemically derived powder. *Materials, 11*(4), 475. [CrossRef]

[47] Feng, Y., Chen, G., Guo, L., Huang, X., Liu, Z., Tian, F., ... & Li, J. (2023). Fabrication of Er: SrF2 transparent ceramics by air pre-sintering and hot isostatic pressing. *Optical Materials, 142*, 114009. [CrossRef]

[48] Laval, M., Moszyński, M., Allemand, R., Cormoreche, E., Guinet, P., Odru, R., & Vacher, J. (1983). Barium fluoride—Inorganic scintillator for subnanosecond timing. *Nuclear Instruments and Methods in Physics Research, 206*(1-2), 169-176. [CrossRef]

[49] Drozdowski, W., Przegiętka, K. R., Wojtowicz, A. J., & Oczkowski, H. L. (1999). Charge traps in Ce-doped CaF_2 and BaF_2. *Acta Physica Polonica A*, 95, 251-258. https://bibliotekanauki.pl/articles/1994795.pdf

[50] Sabharwal, S. C., & Chauhan, A. K. (2002). Effect of lattice oxygen on optical absorption, radiation hardness and thermally stimulated luminescence of BaF2 crystal. *Journal of crystal growth, 240*(3-4), 473-478. [CrossRef]



Heng Liu is a joint master's student of Shanghai Institute of Technology and Shanghai Institute of Ceramics, Chinese Academy of Sciences. His research focuses on the ultrafast BaF2 scintillation ceramics. (Email: 847225629@qq.com)



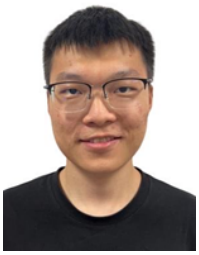
Chen Hu is an Associate Researcher at Shanghai Institute of Ceramics, Chinese Academy of Sciences. His research interests are BaF_2 and Ce:LuAG ceramic scintillators. (Email: huchen@mail.sic.ac.cn)



Jingshan Hou is a professor at Shanghai Institute of Technology. His research focuses on inorganic luminescent materials, phosphors for lighting and displays, optical sensing, and luminescent materials for optical communication and photodetection. He has published over 100 peer-reviewed papers in internationally recognized journals and serves as a reviewer for several international journals in materials science and photonics. (Email: houjingshan@sit.edu.cn)



Ziqiu Cheng is currently a Ph.D. candidate at the Shanghai Institute of Ceramics, Chinese Academy of Sciences. He received his Bachelor of Science degree from the College of Physics, Sichuan University in 2022. His doctoral research focuses on sesquioxide transparent ceramics for solid-state laser and magneto-optic isolator. (Email: chengziqiu20@mails.ucas.ac.cn)



Junhao Ye is currently a Ph.D. candidate at the Shanghai Institute of Ceramics, Chinese Academy of Sciences. He received his Bachelor of Science degree from the College of Physics, Sichuan University in 2022. His doctoral research focuses on sesquioxide transparent ceramics for solid-state laser and magneto-optic isolator. (Email: yejunhao22@mails.ucas.ac.cn)



Tingsong Li is currently a Ph.D. candidate at the Shanghai Institute of Ceramics, Chinese Academy of Sciences. His research focuses on optical and opto-functional ceramics. (Email: litingsong25@mails.ucas.ac.cn)



Dong Huang received his master degree from the college of Materials Science and Engineering, Jiangsu University. Now, he is an assistant engineer of Shanghai Institute of Ceramics, Chinese Academy of Sciences. His research focuses on the Gd_2O_2S ceramics for X-ray and neutron detection imaging. (Email: huangdong@mail.sic.ac.cn)



Yongzheng Fang is a professor and doctoral supervisor at Shanghai Institute of Technology. His research focuses on inorganic luminescent materials, semiconductor lighting and display phosphors, laser lighting, and optoelectronic functional materials. He serves on the editorial boards of academic journals including Glass & Enamel and Journal of Technology. Prof. Fang has published over 100 peer-reviewed papers in internationally recognized journals and has delivered numerous invited talks at academic conferences. (Email: fangyongzheng@sit.edu.cn)



Dariusz Hreniak is a full professor at the Institute of Low Temperature and Structure Research of the Polish Academy of Sciences in Wroclaw, Poland. His research interests are related on optical materials, in particular luminescent materials, and the characterization of luminescent properties of lanthanide ions in glasses, ceramics and nanocomposites. Current interests mainly concern size effects in persistent phosphors. Member of the Editorial Board of the journals Optical Materials (since 2005) and Optical Materials X (since 2021). Scientific secretary of 9 international conferences. Chair and co-chair of scientific committees of 4 international conferences. Co-author of 30 national and international patents and patent applications resulting from R&D projects. (Email: d.hreniak@intibs.pl)



Jiang Li is a professor of Shanghai Institute of Ceramics, Chinese Academy of Sciences (SICCAS). Now he is the deputy director of the transparent ceramics research centre in SICCAS, the associate editors of the Journal of Advanced Ceramics, Journal of Inorganic Materials, and Journal of the American Ceramic Society. Prof. Li's research focuses on laser ceramics, scintillation ceramics, magneto-optical ceramics, ceramic phosphors, and other optical transparent ceramics. He has been selected for four consecutive years as the global top 2% scientists "Lifetime Scientific Impact Rankings" list (2025 edition) released by Stanford University. He was invited to give invited reports in the academic conferences for more than 100 times. He is the coordinator in more than 25 domestic and 8 international collaborative projects so far in the field of transparent and opto-functional ceramics. He produced 501 original papers (10438 Citations, 48 H-index) in refereed journals, 3 co-authored textbooks and 2 co-authored book chapters. (Email: lijiang@mail.sic.ac.cn)